Available online at www.sciencedirect.com
ScienceDirect
Surface & Coatings Technology 202 (2008) 2632–2637
SURFACE & COATINGS TECHNOLOGY
www.elsevier.com/locate/surfcoat

Effects of plastic strain of diamond-like carbon coated stainless steel on the corrosion behavior in simulated body fluid environment

Heon Woong Choi [a,b,*], Kwang-Ryeol Lee [c], Se Jun Park [c], Rizhi Wang [d], Jung-Gu Kim [e], Kyu Hwan Oh [a]

[a] School of Materials Science and Engineering, Seoul National University, Seoul 151-744, Republic of Korea
[b] Department of Materials Science and Engineering, Stanford University, Stanford, CA 94305-2205, USA
[c] Future Convergence Technology Laboratory, Korea Institute of Science and Technology, Seoul 130-650, Republic of Korea
[d] Department of Metals and Materials Engineering, University of British Columbia, Vancouver, BC, Canada V6T 124
[e] Department of Advanced Material Engineering, Sungkyunkwan University, 300 Chunchun-Dong, Jangan-Gu, Suwon 446-746, Republic of Korea

Received 22 March 2007; accepted in revised form 21 September 2007
Available online 9 October 2007

Abstract

We have investigated the effect of plastic deformation of diamond-like carbon (DLC) coated and uncoated stainless steel on the corrosion resistance in a simulated body fluid environment to measure its protective efficiency as a biomedical coating material. We deposited the DLC film on 304 stainless steel specimens by radio frequency plasma assisted chemical vapor deposition(R.F.-PACVD) method, followed by a tensile test to apply plastic strain on the coated specimen. Corrosion behavior in the simulated body fluid environment was studied by a potentiodynamic polarization test. As the tensile deformation progressed, the cracks of the film were observed to be perpendicular to the tensile axis. Further deformation increased both cracking and the spallation. Estimated porosity and corrosion current density increased, and thus the protective efficiency decreased at a strain of 2%. In spite of the degradation, the anti-corrosion properties were significantly improved relative to the uncoated stainless steel. However, a significant increase in porosity and corrosion current density was observed at a strain of 4%. This study showed that increasing the thickness of the Si interlayer of film improved the corrosion resistance with reduction of spallations and cracks.

Keywords: Diamond-like carbon (DLC); Mechanical stability; Tensile test; Potentiodynamic polarization test

1. Introduction

Diamond-like carbon films (DLC) have been considered as a strong candidate for use in blood-contacting applications [1–3] and cell-contacting application [4] due to its excellent mechanical properties [4] and biocompatibility [5]. Thus, various DLC coated implants such as hip replacements [6,7], knee joints [8], orthopaedics, orthodontic implants [9,10] and cardiovascular stents [11–13] are being intensely investigated. Among these investigations, the importances of stents have grown rapidly because it can prevent a sudden death caused by myocardial infarction. In general, the diameter of the stent is enlarged by at least a factor of two after expanding in the vein. Furthermore, the stent should endure the environmental pressure in the range of 10–20 atm in the human body that induces stenocardia. Thus, as a medical device, the stent should have sufficient structural strength in addition to the biocompatibility [12]. Typically, two kinds of materials are used for stents. One is nitinol (NiTi), and the other is stainless steel. Nitinol alloys have been widely used in the stents due to their excellent shape memory properties, superelasticity and good corrosion resistance with the formation of a thin passive film [14] because NiTi alloys that possess shape and super-elastic properties are of interest in spindal deformity correction and shape recovery inside human body allows for less traumatic gradual correction while obviating the needs for multiple surgeries [15]. However, one should note that the Ni content in the alloy is more than 50 at.%. Nickel is an element that is

* Corresponding author. School of Materials Science and Engineering, Seoul National University, Seoul 151-744, Republic of Korea.
E-mail address: joiner03@snu.ac.kr (H.W. Choi).

0257-8972/$ - see front matter © 2007 Elsevier B.V. All rights reserved.
doi:10.1016/j.surfcoat.2007.09.046

known to be toxic and allergenic, and the release of Ni ions in implants takes place during the corrosion in the human body [16]. In addition, corrosion due to damaged passive films accelerates the release of Ni ions in human body. Stainless steel is also a common material for mechanical heart valves or orthopaedic implants [13,17]. Although, it has widespread usages for heart valve purpose, stainless steel is not the best material since it contains harmful poisonous element such as a Cr or Ni. In both cases of materials of stent, it is essentially required to coat the stent surface with a corrosion resistant layer to prevent release of potentially harmful metal ions [18].

DLC films have been considered as a protective layer for medical implant materials [19] that can meet the requirements of suppressing the harmful release of ions, wear debris formation, and undesirable biological reactions with the surrounding tissue. However, DLC films have a disadvantage because of their poor adhesion on metal substrate. This is either due to the lack of chemical affinity against metal substrate which cannot form carbide bonding between the film and substrates [20] or due to compressive residual stresses up to 10 GPa which can induce a delamination of the film [21]. In order to enhance their practical application for medical devices, the stability of DLC coatings should be investigated under the deformation of substrate, since cracking and spallations of the films can accelerate the release of harmful ions in human body. In addition, the body fluid is a corrosive environment conditions which can also lead not only crevice attacks but also pitting for metal alloys [22]. Thus in the present work, we deposited the DLC film on 304 stainless steel tensile specimens and imposed tensile strains. Anticorrosion behaviors of the specimen were evaluated in the simulated body fluid.

2. Experimental

The 304 stainless steel substrates were electrochemically polished to obtain smooth surfaces followed by full cleanings with trichloroethylene, acetone and ethanol and finally dried with Ar gas. After that, the 304 stainless steel and p-type Si (100) wafer substrates were introduced into chamber for deposition of DLC films. We synthesized the DLC film with a residual stress of 0.9±0.2 GPa and a hardness of 10.0± 1.0 GPa on a 500±10 μm thick Si wafer and on 304 stainless steel substrates by R.F.-PACVD using benzene as the precursor gas. The thickness of the film was kept constant (1.0±0.1 μm) for all specimens. Details of the deposition equipment are described elsewhere [23]. In order to focus on the interfacial characteristics between the substrate and the film, we deposited the films with the same thickness and the same properties. Before the film deposition, the substrate was sputter cleaned by Ar plasma at the bias voltage −600 V for 60 min. Thin Si interlayers with thicknesses ranging from 19 to 84 nm were then deposited to improve the adhesion of the DLC layer and to

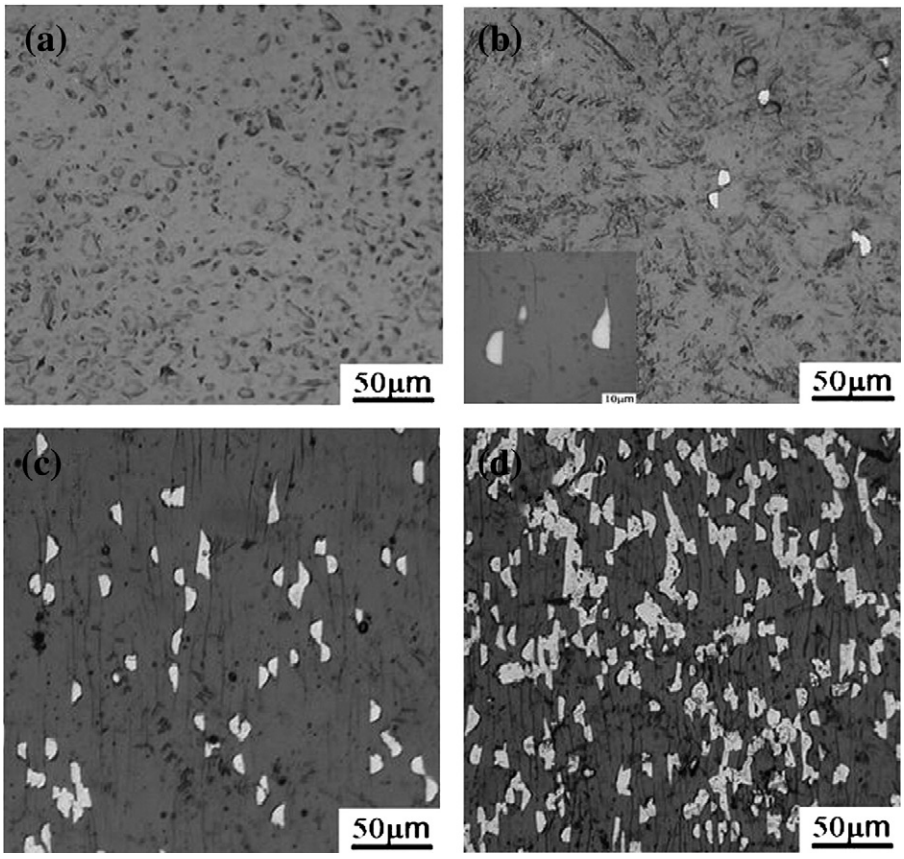

Fig. 1. SEM microstructure of the sample surface after imposing tensile strain of (a) 2%, (b) 4%, (c) 6% and (d) 8%.

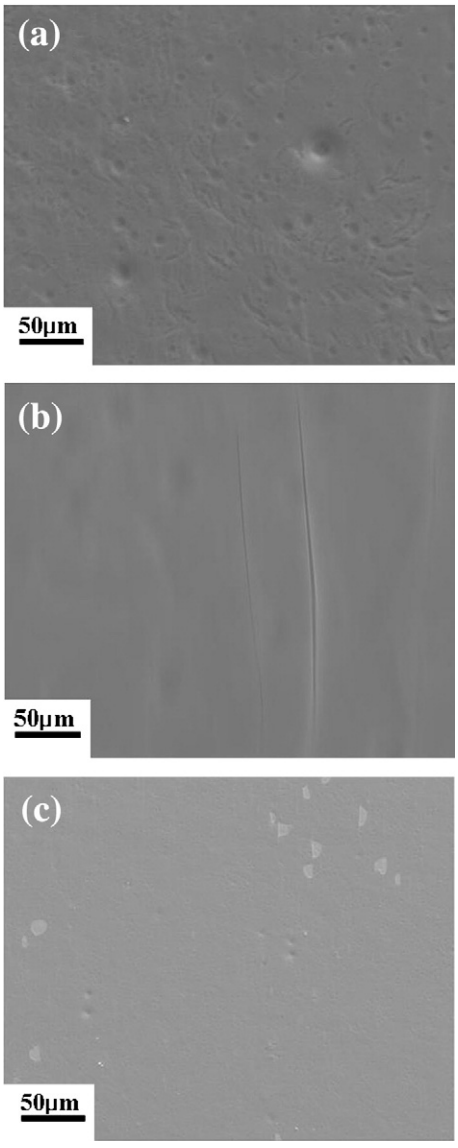

Fig. 2. SEM microstructure of the sample surface with Si interlayer thickness of 98 nm after imposing tensile strain of (a) 2%, (b) 3% and (c) 4%.

investigate the effects of interlayer thickness on the corrosion behaviors in simulated body conditions.

We performed the tensile test using a micro-tensile tester with 0.2 mm/min strain rate. Strain was varied from 2 to 8% to perform various plastic strain effects on the DLC films. After the tensile test, the specimen surface was observed by an optical microscope and a scanning electron microscope. Potentiodynamic polarization test was determined with an EG & G Princeton Applied Research Model 273A potentionstat and carried out with enhanced adhesion of film by controlling the Si interlayer thickness to 98 nm in a 0.89 wt.% NaCl solution of pH 7.4 at temperature of 37 °C that was thoroughly deaerated by high purity nitrogen gas for 1 h before the immersion of the sample and continuously purged during the test. This solution designed to simulate human body conditions. The exposed coating area was 1.0 cm^2. Saturated calomel electrode (SCE) and pure graphite were used for reference and counter electrodes, respectively. Prior to the beginning of the potentiodynamic polarization test, the samples were kept in solution for 6 h in order to set up the open circuit potential (OCP). The current between the counter electrode and the specimen as a function of the potential was measured, obtaining the anode polarization curve. The potential of the electrode was swept at a rate of 0.166 mV/s from the initial potential of −250 mV versus E_{corr} to the final potential of 1500 mV. Scanning electron microscopy (SEM) was also used to investigate the corroded surfaces morphology of tested samples. Porosity can indicate an obvious fracture path for adhesion failure [24,25]. Matthes et al. [24] suggested that an empirical equation to evaluate the porosity (P) of the films and protective efficiency are;

$$P = \frac{R_{\text{pm (substrate)}}}{R_{\text{p (coating/substrate)}}} 10^{-|\Delta E_{corr}/\beta_a|} \quad (1)$$

where P is the total coating porosity, R_{pm} the polarization resistance of the substrate material, R_p the calculated polarization resistance of the coated system, and ΔE_{corr} the potential difference between the bare substrate steel and the corrosion potentials of the coated steel. Calculated polarization resistance of the coated system is

$$R_p = (\beta_a \times \beta_c)/\{2.3 \times I_{corr} \times (\beta_a + \beta_c)\} \quad (2)$$

where β_a is the anodic Tafel constant and β_c is the cathodic Tafel constant. Protective efficiency (P_i) of the film is determined from the polarization curve by Eq. (3) [25]

$$P_i = 100\left(1 - \frac{i_{corr}}{i^0_{corr}}\right) \quad (3)$$

where i_{corr} and i^0_{corr} are that the corrosion current densities in the presence and absence of the coating, respectively. In addition, in the anode polarization curve, the critical passivation current density is proportional to the area of metal exposed to the chemical solution. Lower passivation current densities correspond to a higher corrosion resistance of the specimen [26]. Therefore, the anode polarization curve was measured for

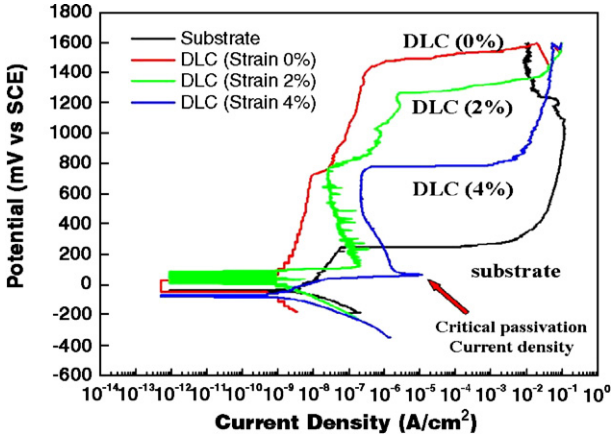

Fig. 3. Potentiodynamic polarization test curves in deaerated 0.89% NaCl solution at 37 °C (pH=7.4).

Table 1
Results of potentiodynamic polarization test curves in deaerated 0.89% NaCl solution at 37 °C (pH=7.4)

Strain (coated DLC)	E_{corr} (mV)	i_{corr} (nA/cm^2)	β_a (V/decade)	β_c (v/decade)	R_p ($\times 10^3$ Ω cm^2)	Protective efficiency (%)	Porosity
Bare substrate	−33.9	6.557	0.2981	0.0693	3726.2217	–	–
0%	−32.55	0.312	0.2284	0.1425	122441.5576	95.25	0.0301
2%	−29.86	1.126	0.4851	0.1137	35566.7122	82.83	0.1015
4%	−69.32	4.720	0.1000	0.1041	4698.2691	28.02	0.6033

illustrating of protective efficiency on various plastic strained DLC films.

3. Results and discussion

Fig. 1 shows the various plastic strain applied DLC film with 19 nm of Si interlayer thickness on 304 stainless steel. Fig. 1(a) clearly shows no crack formation at 2% strain. However, as increasing of strain from 4% to 8%, the crack formation and spallations of film were simultaneously produced. It is also noticed that spallations of the film occurred with the crack propagation, although the number density of the spallations is very low. Further increasing the strain to 6% and 8% increased both the crack density and the number of the spallated area as shown in Fig. 1(c) and (d), respectively. However, when increased the Si interlayer thickness from 19 to 98 nm, we observed the decreasing of crack formation and spallations as shown in Fig. 2. When the Si interlayer thickness of 19 nm, we observed a number of crack and the spallations on 2% strained DLC film but by controlling the Si interlayer thickness to 98 nm, we observed the absence of crack formation and spallations while crack initiation observed at 3% strained film as shown in Fig. 2b. In the present experiment, the spallation area in the film was compared to characterize the adhesion of the DLC coating between the 19 nm and 98 nm Si interlayer thickness of specimens at the same strain with considering previous works [23]. Thus, the adhesion of the film was improved with increasing Si interlayer thickness. The present results are consistent with those of the scratch test for DLC films on tool substrates under similar deposition conditions [29].

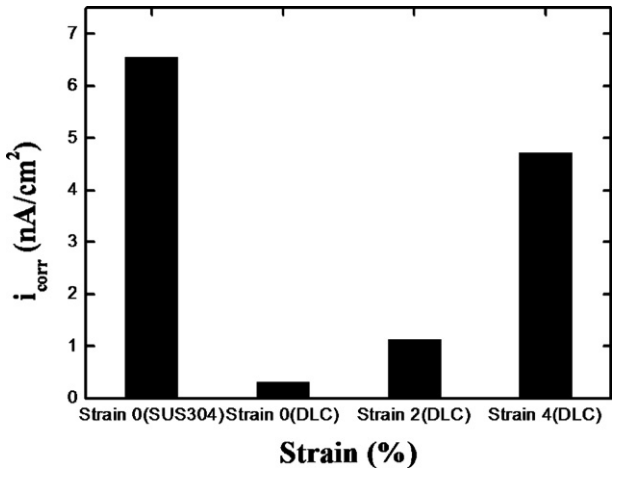

Fig. 4. Corrosion current densities for the SUS 304 substrate and various strained DLC coated specimens with a Si interlayer thickness of 98 nm.

With the aim of studying the protection abilities and stabilities on localized corrosion of coating, potentiodynamic polarization measurements were carried out in simulated body fluid conditions at various strains with a Si interlayer thickness of 98 nm. The potentiodynamic polarization curves for the DLC films are shown in Fig. 3, and the measured corrosion potential (E_{corr}) in terms of mV VS SCE calculated from the intersection of the Tafel slopes, corrosion current density (i_{corr}) which also obtained from the intersection of the Tafel slopes and matched to the value of current density in x-axis, protective efficiency (P_i) and porosity (P) are given in Table 1. It clearly shows that the passive film was formed on all the specimens and demonstrates good corrosion resistance of the DLC coated specimens because passivity of formation in diamond-like carbon film can be interpreted using wide passive potential range and low current density. By reduction of exposure area with DLC film which have less porosity or delaminated area between the corrosive solution and the coated substrate, the corrosion speed can be reduced [22] as summarized in Table 1. Fig. 4 shows the corrosion current density obtained from the potentiodynamic polarization curve. As shown in Fig. 4, the corrosion current density improved with all of the DLC coatings compared to the bare SUS 304 substrate and shows that the passive region was produced on the all the DLC films. Increasing the plastic strain of DLC films resulted in the deterioration of both the corrosion current density and the passive region, but the DLC coated specimens still showed better characteristics than the bare substrate. This indicates that the unstrained DLC coating with fewer pores makes the substrate more passive than strained coatings and an SUS 304 substrate with more pores. The electrochemical determination gives a porosity of 0.0301 for the unstrained DLC film, 0.101 for 2% strained DLC film and 0.6033 for 4% strained DLC film. These pores can weaken the interface and provide a path for the release of metallic ions [24]. A similar trend of corrosion density and passivity region was also observed. The corrosion density was 6.55 nA/cm^2 for the uncoated sample, 0.31 nA/cm^2 for the unstrained sample, 1.12 nA/cm^2 for the 2% strained sample and 4.72 nA/cm^2 for the 4% strained sample. The corrosion current density can indicate the protective efficiency. The highest protective efficiency was 95.25% for the unstrained DLC film which was well passivated, with a wide passive potential range and low passive current density. The coated samples showed an improved protective efficiency up to a plastic strain of 2%. This protective efficiency is related to crack formation, spallations of the film and porosity in DLC films. The lower measured protective efficiency, the higher crack formation, spallations of film and porosity as shown in Table 1. Fig. 5 shows the surface morphologies of the specimens after the potentiodynamic polarization test. Increasing

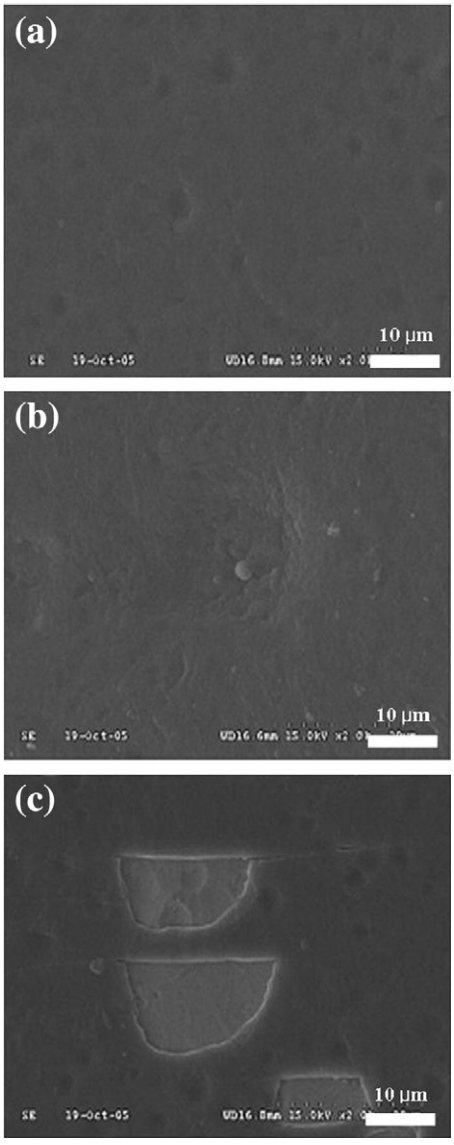

Fig. 5. The surface morphologies of the specimen after potentiodynamic polarization test at (a) 0% (b) 2% and (c) 4% which all controlled Si buffer layer thickness to 98 nm to enhance the adhesion.

strain resulted in more plastic deformation of the DLC films, causing cracking and spallations and exposing the metal substrate. This significantly increases the porosity due to crack formation and cause the deterioration of the critical passivation current density because the critical passivation current density is proportional to the area of metal exposed to the chemical solution [26–28]. This is similar to the corrosion protective ability and durability of coatings for real applications. However, this study has several limitations to apply in reality because artificial ageing is far from being relevant to in vivo ageing due to the lack of proteins and its byproducts which have been found to substantially change the surface profile of the materials. In these applications, calcifications of proteinaceous species showed to be adsorbed onto the surface after exposure to the host environment which has been found to be the predominant mechanism of ageing. Thus, there might be the difference when evaluate the corrosion behavior in vivo. But this study showed the effects of Si buffer layer thickness and plastic strain on DLC film in simulated body conditions.

4. Conclusions

We studied the corrosion resistance of diamond-like carbon film by tensile and potentiodynamic polarization tests in simulated body conditions. We observed that the adhesion of DLC film was enhanced by increasing the thickness of Si buffer layer. When 2% of strain was applied to the sample, no cracking was observed. However, there was a 13% decrease of protective efficiency due to increasing porosity in the film. At a strain of 4%, both cracking and spallations developed, and there was a significant reduction of protective efficiency. Nevertheless, the coated samples show better protective efficiencies than the uncoated sample.

Acknowledgements

This research was supported by a grant (code number: 06K1501-01600) from ‘Center for Nanostructured Materials Technology’ under ‘21st Century Frontier R&D Programs’ of the Ministry of Science and Technology, Korea and the authors are thankful for Mr. Markus Ong, Department of Material Science and Engineering of Stanford University for friendly advice.

References

[1] S. Logothetidis, M. Gioti, S. Lousinian, S. Fotiadou, Thin solid films 482 (2005) 126.
[2] T.I.T. Okpalugo, A.A. Ogwu, P.D. Magguire, J.A.D. Mclaughlin, Biomaterials 25 (2004) 239.
[3] M.I. Jones, I.R. McColl, D.M. Grant, K.G. Parker, T.L. Parker, Diamond Relat. Mater. 8 (1999) 457.
[4] K.-R. Lee, K.Y. Eun, K.-M. Kim, K.-C. Choi, Surf. Coat. Technol. 76-77 (1995) 786.
[5] L.J. Yu, X. Wang, X.H. Wang, X.H. Liu, Surf. Coat. Technol. 128-129 (2000) 484.
[6] S. Reuter, B. Weвkamp, R. Bűscher, A. Fischer, B. Barden, F. Lőer, V. Buok, Wear 261 (2006) 419.
[7] F. Platon, P. Fournier, S. Rouxel, Wear 250 (2001) 227.
[8] J.I. Oñate, M. Comin, I. Braceras, A. Garagorri, J.L. Peris, J.I. Alava, Surf. Coat. Technol. 142-144 (2001) 1056.
[9] D.P. Dowling, P.V. Kola, K. Donnelly, T.C. Kelly, K. Brumitt, L. Lioyed, R. Eloy, M. Therin, N. Weill, Diamond Relat. Mater. 6 (1997) 390.
[10] S. Kobayashi, Y. Ohgoe, K. Ozeki, K. Sato, T. Sumiya, K.K. Hirakuri, H. Aoki, Diamond Relat. Mater. 14 (2005) 1094.
[11] J.H. Sui, W. Cai, Diamond. Relat. Mater. 15 (2006) 1720.
[12] J.H. Sui, W. Cai, Surf. Coat. Technol. 201 (2007) 5121.
[13] N. Ali, Y. Kousar, T.I. Okpalugo, V. Singh, M. Pease, A.A. Ogwu, J. Gracio, E. Titus, E.I. Meletis, M.J. Jackson, Thin solid films 515 (2006) 59.
[14] Z. Xu, P.R. Almond, J.O. Deasy, Int. J. Radiat. Oncol. Biol. Phys. 36 (1996) 933.
[15] P.K. Chu, Surf. Coat. Technol. 201 (2007) 5601.
[16] Z.D.J. Wever, A.G. Veldhuizen, J. Vries, H.J. Busscher, D.R.A. Uges, J.R. van Horn, Biomaterials 19 (1998) 761.
[17] P.D. Maguire, J.A. McLaughlin, T.I.T. Okpalugo, P. Lemoine, P. Papakonstantinou, E.T. McAdams, M. Needham, A.A. Ogwu, M. Ball, G.A. Abbas, Diamond. Relat. Mater. 14 (2005) 1277.

[18] H. Hara, M. Nakamura, J.C. Palmaz, R.S. Schwarts, Advance Drug Deliv. 58 (2006) 387.
[19] R. Hauert, Diamond. Relat. Mater. 12 (2003) 583.
[20] K. Oguri, T. Arai, Surf. Coat. Technol. 47 (1990) 710.
[21] S.J. Park, K.-R. Lee, D.-H. Ko, K.Y. Eun, Diamond Rel. Mater. 11 (2002) 1747.
[22] H.-G. Kim, S.-H. Ahn, J.-G. Kim, S.J. Park, K.-R. Lee, Thin solid films 475 (2005) 291.
[23] H.W. Choi, K.-R. Lee, R. Wang, K.H. Oh, Diamond Relat. Mater. 15 (2006) 38.
[24] B. Matthes, E. Brozeit, J. Aromaa, H. Ronkainen, S.P. Hannula, A. Leyland, A. Matthews, Surf. Coat. Technol. 49 (1991) 489.
[25] Y.J. Yu, J.G. Kim, S.H. Cho, J.H. Boo, Surf. Coat. Technol. 162 (2003) 161.
[26] M. Yatsuzuka, J. Tateiwa, H. Uchida, Vacuum 80 (2006) 1351.
[27] D.O. Sprowls, "Corrosion", Metals Hand Book Ninth Edition, vol 12, ASTM International, 1987, p. 217.
[28] ASTM G3-Standard Recommended Practice for Conventions Applicable to Electrochemical Measurements in Corrosion Tests, 1989.
[29] Y.H. Jun, J.-Y. Choi, K.-R. Lee, B.-K. Jeong, S.-K. Kwon, C.-H. Hwang, Thin solid films 377-378 (2003) 233.